Antibacterial and Cytotoxicity Effect of Flavokawain B Loaded Silver Nanoparticles

[1,2] Muhammad Nadeem Akhtar*, [2]Liew Syn Yee, [2]Seema Zareen, [1]Tayyaba Shabir and [3]Sarosh Iqbal
[1]*Department of Chemistry, Faculty of Science, Ghazi University, Dera Ghazi Khan.*
[2]*Faculty of Industrial Sciences & Technology, University Malaysia Pahang, Lebuhraya Tun Razak 26300, Kuantan Pahang, Malaysia.*
[3]*Department of Applied Chemistry, Government College University, Faisalabad 38000, Pakistan.*
nadeemupm@gmail.com*

(Received on 15th June 2023, accepted in revised form 7th November 2023)

Summary: Silver nanoparticles (Ag NPs) are used in sterilizing nanomaterials, medical products, textiles, food storage bags, and personal care products. Ag NPs exhibited significant antibacterial activity due to the sustained release of free Ag. Flavokawain B (FKB) is a natural chalcone extracted from the roots of the kava-kava plant *Piper methysticum*. In this study, Ag NPs were synthesized by the chemical method using hydrazine hydrate and poly (vinyl alcohol) as reducing and stabilizing agents, respectively. FKB-loaded Ag NPs showed a red shift and were positioned at 421 nm, indicating Ag NPs presence. The FTIR spectrum confirmed the presence of the aromatic compound's functional groups (at different absorption bands). The XRD pattern indicated the crystalline nature of the loaded Ag NPs with face-centered cubic (fcc) Ag crystals. SEM image revealed the crystalline nature of FKB-loaded Ag NPs. FESEM image revealed the loading of Ag NPs on the clear and flat surface of FKB, and a spherical shape of Ag NPs with an average size of 60 nm was obtained. The minimum inhibitory concentration (MIC) of AgFKB against Gram-negative bacteria, *Escherichia coli* and *Pseudomonas aeruginosa* was found to be 100 µg/mL. However, 100 µg/mL of FKB discs did not show any inhibition zone in the activity. These findings indicated the improved antibacterial activity of FKB-loaded Ag NPs (Ag-FKB).

Keywords: Silver nanoparticles, Flavokawain B, Flavokawain B loaded silver nanoparticles, Antibacterial activity, Gram-negative bacteria.

Introduction

The fundamental premise of nanotechnology was introduced by Richard Feynman in 1959 at the American Physical Society's annual conference [1]. Nowadays, nanotechnology is an emerging field of modern research that involves synthesizing and manipulating NPs with sizes ranging from approximately 1 to 100 nm [2-4]. Nanoparticles exhibit unique and intriguing characteristics owing to their nanoscale, huge surface areas with freely dangling bonds, and more reactivity than their bulk counterparts [5]. Among different types of NPs, the most promising one is metallic NPs, which have excellent antibacterial properties because of their large surface area-to-volume ratio [6, 7]. There are several methods used to synthesize NPs such as biological, chemical, physical, and enzymatic [8].

Ag NPs make up 56% of all the nanoparticles in the world [9, 10]. Ag NPs typically have sizes under 100 nm and contain 20 to 15,000 silver atoms [11, 12]. Ag NPs have enhanced properties compared to their parent materials and are applicable in various fields, especially in biomedical science [13-15]. The Ag NPs have gained much interest among the noble metallic NPs due to their special properties such as the most significant antibacterial, antifungal, antiviral, and anti-inflammatory activities, good conductivity, chemical stability, and catalytic properties which can be incorporated into cosmetic products, composite fibers, electronic components, cryogenic superconducting materials, and food industry [2, 16, 17]. The most important application of Ag and Ag NPs is in the medical industry such as tropical ointments that are used to prevent infection against burn and open wounds [18, 19].

FKB is a naturally occurring chalcone that can be isolated through the root extracts of the kava-kava plant (*Piper methysticum*) [20, 21]. It can be synthesized chemically to increase the yield. This compound is a promising candidate as a biological agent, as it is reportedly involved in a wide range of biological activities. FKB was demonstrated to have a high cytocidal effect against lung, prostate, uterine, oral, breast, bone, and synovial cancer cells, with negligible toxicity toward normal cells [22]. Furthermore, FKB was reported to have antitumorigenic effects in several cancer cell lines in vitro. Apart from that, FKB was also found to inhibit metastasis, as evaluated by clonogenic assay, bone marrow smearing assay, real-time polymerase chain reaction, western blot, and proteome profiler analysis. FKB may serve as a promising anticancer agent, especially in treating breast cancer [21, 23-28]. FKB-loaded Ag NPs have not, as far as we are aware, been used as a bacterial inhibitor. This study is the first investigation to report the use of FKB-loaded Ag NPs as

*To whom all correspondence should be addressed.

antibacterial agents against gram-negative bacteria. The present study aims to synthesize and characterize the FKB-loaded Ag NPs. Disc Diffusion technique is employed to study its antibacterial activity against *E. Coli* and *P. aeruginosa*.

Experimental

Materials

All the chemicals and solvents used were of analytical grade and were used without any further purification. Methanol, 4',6'-dimethoxy-2'-hydroxy acetophenone, benzaldehyde, hydrochloric acid, brine, sodium sulfate, ethyl acetate, hexane, hydrazine hydrate, ethanol, and silver nitrate were purchased from Sigma Aldrich.

Methods

Synthesis of Silver Nanoparticles: 50 mL methanol was mixed with distilled water in a 500 mL round bottle flask, and it was left for 15 minutes at room temperature. 5.0 g (25.5 mmol) 4',6'-dimethoxy-2'-hydroxy acetophenone was poured into the round bottle flask and stirred for a further 10 minutes. 2.04 mL (20.0 mmol) of freshly distilled benzaldehyde was added to the mixture and stirred for another 24 hours at room temperature. The crude product was then transferred into a 500 mL separating funnel. 200 mL of distilled water was added. The mixture was then neutralized by adding 2 to 3 mL of hydrochloric acid. The product was extracted three times from the aqueous layer using 150 mL ethyl acetate. The organic layer was successively washed with brine and dried over anhydrous sodium sulfate. Finally, the crude product was purified by flash column chromatography using ethyl acetate and hexane as eluents and it was recrystallized in methanol [29].

Preparation of Flavokawain B Solution: To prepare 100 mL of 3.23 mg/mL FKB solution, 0.323 g was weighed and dissolved in 100 mL of ethanol [27, 30].

Synthesis of Poly Vinyl Alcohol (PVA) Stabilized Ag NPs: 0.1% w/v PVA solution was prepared by dissolving 0.1 g PVA in distilled water to a final volume of 100 mL [31]. 1% v/v hydrazine hydrate solution was prepared by dissolving 1.8 mL of hydrazine hydrate in distilled water to a final volume of 100 mL. 0.1 mM silver nitrate solution was prepared by dissolving 1.7 mg silver nitrate in distilled water to a final volume of 100 mL [32]. 100 mL PVA solution (0.1% w/v) was added to 100 mL of silver nitrate solution (0.1 mM) with constant stirring. Hydrazine hydrate solution (1% v/v) was added dropwise to obtain a pale yellow colloidal solution [33].

Flavokawain B Loading on PVA Stabilized Ag NPs (Ag PVAFKB): 100 mL of both Ag PVA colloid and FKB solution (3.23 mg/mL) were mixed and stirred using a hot plate for 24 hours at room temperature. This colloidal solution was then centrifuged two times for 30 minutes at 15,000 rpm to obtain the pellets [33].

Synthesis of Flavokawain B Loaded Ag NPs: After adding 5 drops of hydrazine hydrate solution (1% v/v) to the mixture of silver nitrate solution (10^{-4} M) and PVA solution (0.1 % w/v), the colorless mixture was changed to pale yellow colloidal solution as shown in Fig 1. This indicates the formation of Ag NPs in the solution. Ag NPs show a yellowish-brown color in aqueous solution because of the excitation of surface plasmon vibrations in the particles [34]. The Ag-PVA colloid was further added with FKB solution (3.23 mg/mL) and stirred for 24 hours at room temperature for effective loading of the FKB onto the PVA-stabilized Ag NPs [33]. The formation of AgFKB NPs was further confirmed by Ultraviolet-Visible (UV-Vis) Spectroscopy, Fourier Transform Infrared Spectroscopy (FTIR), X-Ray Diffraction (XRD) analysis, Scanning Electron Microscopy (SEM), and Field Emission Scanning Electron Microscopy (FESEM). Fig.1. presents an illustration of a mixture of Ag nitrate solution PVA solution and pale-yellow colloidal solution.

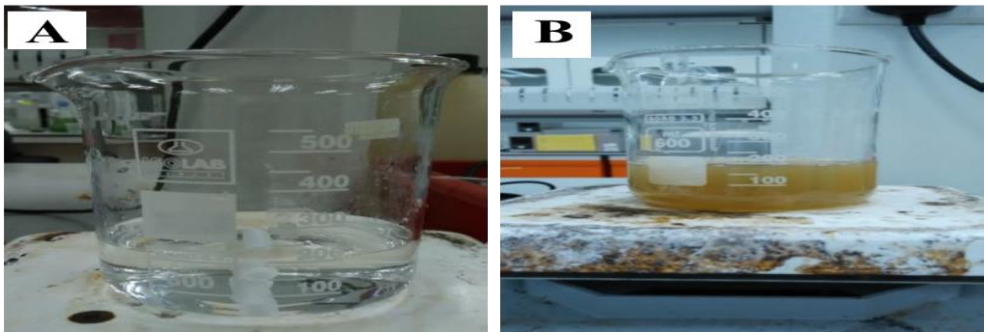

Fig. 1: (A): Mixture of Ag nitrate solution (10^{-4} M) and PVA solution (0.1 % w/v); (B): Pale yellow colloidal solution after adding 5 drops of hydrazine hydrate solution (1% v/v).

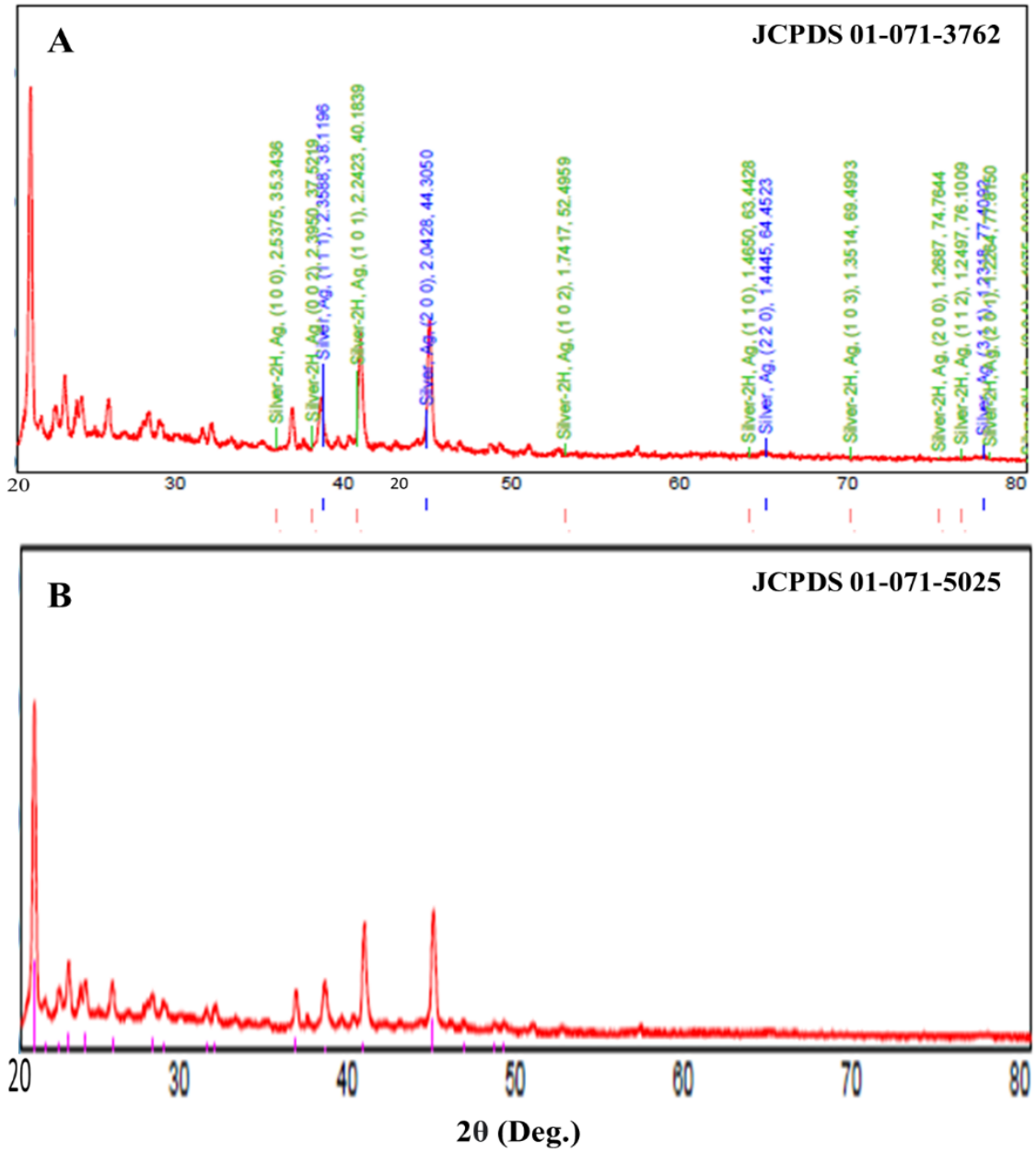

Fig. 2: XRD pattern of FKB Loaded Ag NPs (A and B).

Scanning Electron Microscopy (SEM) Analysis

The morphology of AgFKB NPs cannot be studied clearly because the maximum magnification that can be reached are 3000X and 5000X as shown in Fig. 3. (A) and (B) corresponding to the width of 2 µm and 1 µm, respectively that can be imaged in a scanning mode. However, the images revealed the crystalline structure of FKB, indicating the presence of FKB in the synthesized AgFKB NPs. The morphology was further studied using Field Emission Scanning Electron Microscopy (FESEM). Fig 3. presents an illustration of SEM images. The average particle size of synthesized FKB-loaded Ag NPs was 72 nm calculated using ImageJ software [41, 42].

Field Emission Scanning Electron Microscopy (FESEM) Analysis

The morphology of FKB-loaded Ag NPs was studied using Field Emission Scanning Electron Microscopy at a magnification of 5000X. To confirm the loading of FKB on Ag NPs, the morphology of pure FKB and the synthesized product FKB-loaded Ag

NPs were compared. FESEM image of pure FKB is shown in Fig 4 (A) indicating the crystalline nature, and most importantly the clear and flat surface. On the other hand, the FESEM image of FKB-loaded Ag NPs shown in Fig 4 (B), indicates the visible Ag NPs on the surface of FKB. The Ag NPs obtained are spherical in shape with an average size of 60 nm [43]. This confirmed that FKB was successfully loaded on the Ag NPs. The enhanced effect of FKB-loaded Ag NPs was further studied by observing their antibacterial effect in comparison to the effect of the pure FKB. Fig 4 presents an illustration of FESEM images.

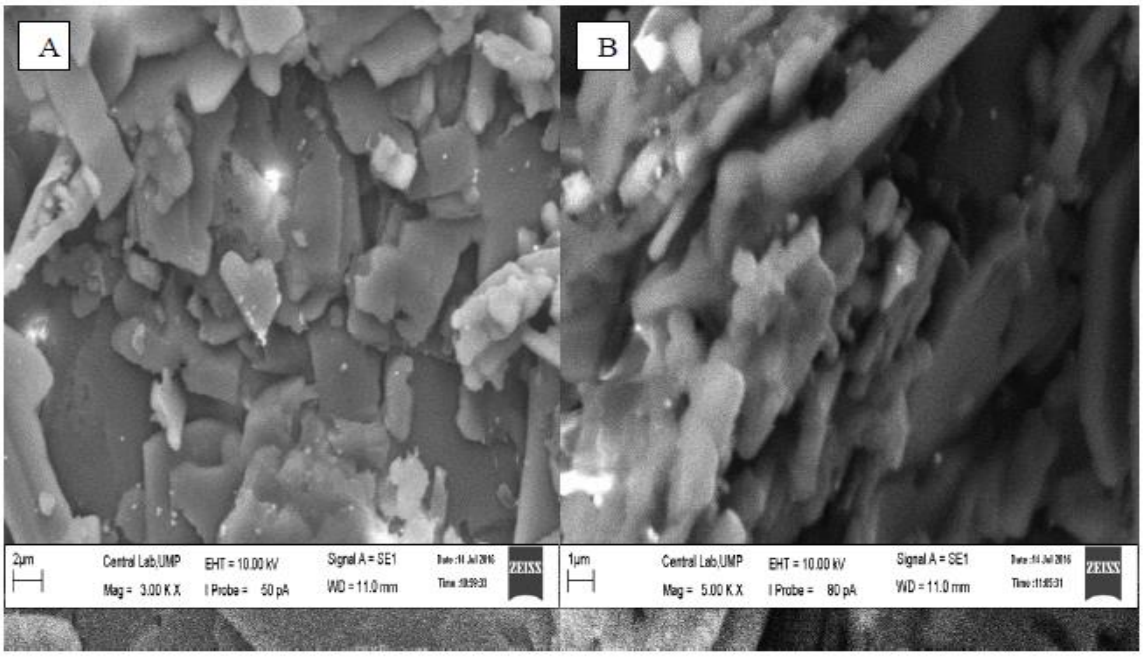

Fig. 3: SEM images of FKB-loaded Ag NPs recorded at 3000X (A) and 5000X (B) of magnification.

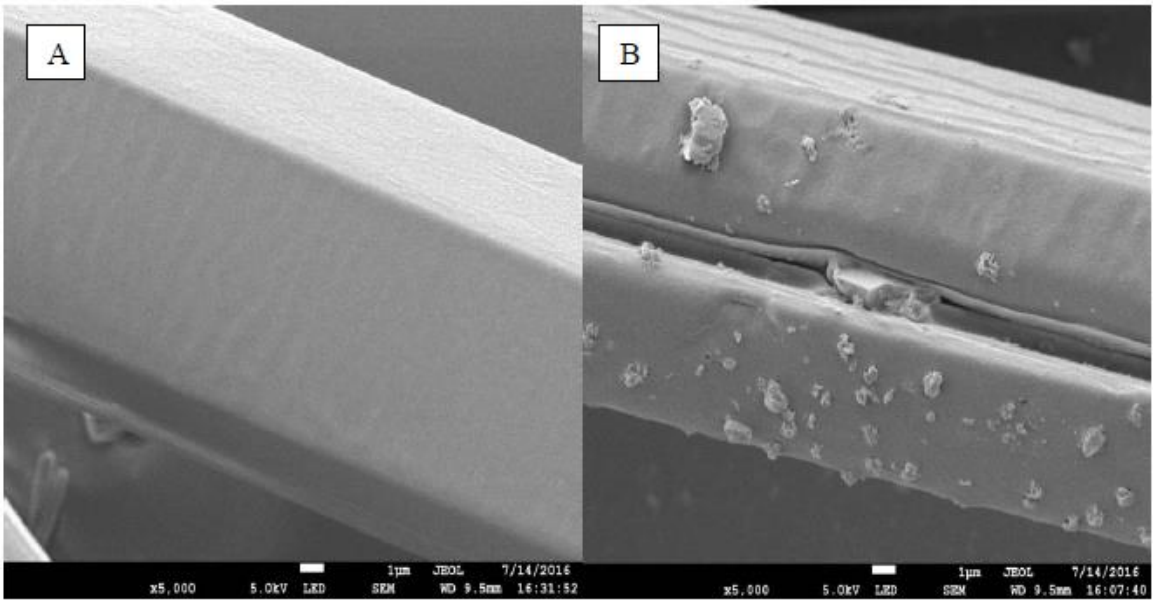

Fig. 4: (A): FESEM image of FKB; (B): FESEM image of FKB loaded Ag NPs.

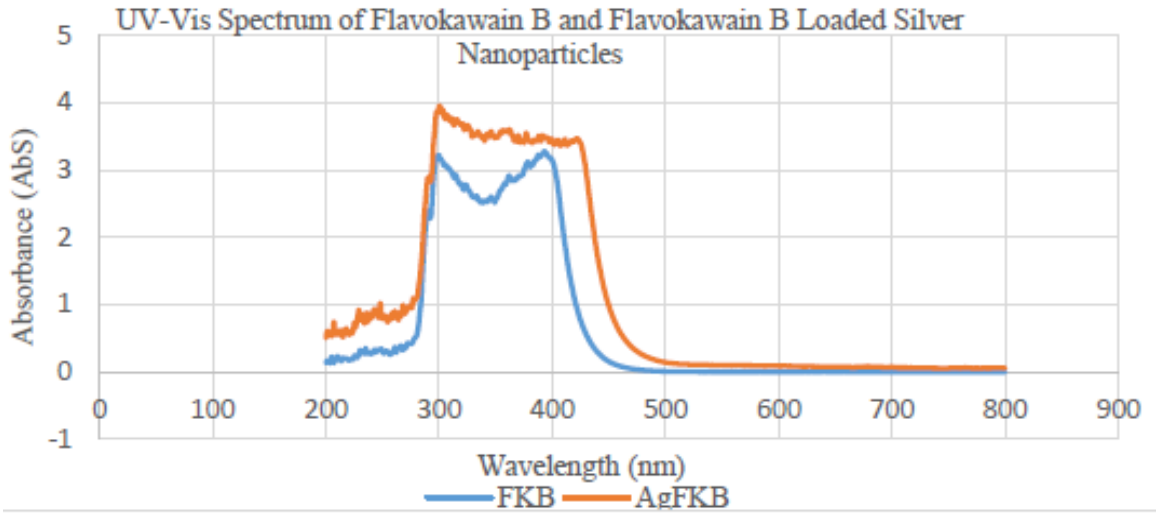

Fig. 5: UV-visible spectra of FKB and FKB loaded Ag NPs.

Ultraviolet-Visible (UV-VIS) Spectroscopy Analysis

UV-Visible spectroscopy is technique for the structural characterization of NPs. It is used to confirm the initial formation of NPs. Metal NPs' optical absorption spectra are dominated by Surface Plasmon Resonance (SPR), which shifts to the longer wavelength when particle size increases [33]. SPR is due to the combined oscillation of free electrons of Ag NPs in resonance with light waves [36]. According to H. H. Rashid, Ag NPs have a typical absorption band in the 350 nm to 450 nm region [44]. To understand the interaction of FKB with Ag NPs, the UV-visible spectra of FKB and FKB-loaded Ag NPs (AgFKB) were recorded. The difference in the UV-Vis spectra can be observed. According to Fig 5, the UV-visible spectrum of FKB shows two characteristic absorption bands centered at 300 nm and 393 nm. However, when FKB was loaded on Ag NPs, the peaks were observed at 300 nm and 421 nm. The SPR band originating from the AgNPs in the AgFKB NPs showed a red shift and was positioned at 421 nm [45]. This confirmed that FKB is successfully loaded onto the AgNPs as shown below in Fig 5.

Fourier Transform Infrared (FTIR) Spectroscopy Analysis

The main purpose of FTIR spectroscopy in metal NPs characterization is to detect chemical species that interact with the particle surface [46]. According to Fig 6, the FTIR spectrum of FKB-loaded Ag NPs displayed absorption band at 3415.28 cm^{-1} and 3468.13 cm^{-1} (O-H stretch), 1632.15 cm^{-1} (α, β-unsaturated carbonyl group), 1586.34 cm^{-1} (aromatic C=C stretch), and 1219.37 cm^{-1} (C-O-C ether linkage). The C-H stretching occurs above 3000 cm^{-1} which confirmed the presence of aromatic compound [47]. Hence, it can be concluded that the aromatic compound, FKB is present in the synthesized AgFKB NPs as all the functional groups are indicated by the peaks of the spectrum.

Antibacterial Activity

The inhibition zone of FKB and AgFKB was determined against *E. Coli* and *P. aeruginosa*. All of the Gentamicin (10 g) discs had action against *E. Coli* and *P. aeruginosa* with inhibition zones measuring 20 mm in diameter, as shown in Table 1.

The MIC of AgFKB was determined to be 100 µg/mL as demonstrated in the Test. Diffusion results of FKB and AgFKB against *E. Coli* and *P. aeruginosa* are shown in the supplementary material. All the 100 µg/mL AgFKB discs showed an inhibition zone of 6 mm in diameter in the activity against *E. Coli* and *P. aeruginosa.* 25, 50, and 75 µg/mL AgFKB discs did not show any inhibition zone in the activity. On the other extreme, 100 µg/mL FKB discs did not show any inhibition zone in the activity against *E. Coli* and *P. aeruginosa*. These showed the improved activity of AgFKB against pure FKB.

Table-1: Antibacterial activity of FKB and AgFKB against Gram-negative bacteria.

Strains	Nature	Inhibition zone (mm)							
		Positive control (Gentamicin 10 µg)	FKB (µg/mL)				AgFKB (µg/mL)			
			25	50	75	100	25	50	75	100
E. coli	Gram-negative	20 mm	0	0	0	0	0	0	0	6
P. aeruginosa		20 mm	0	0	0	0	0	0	0	6

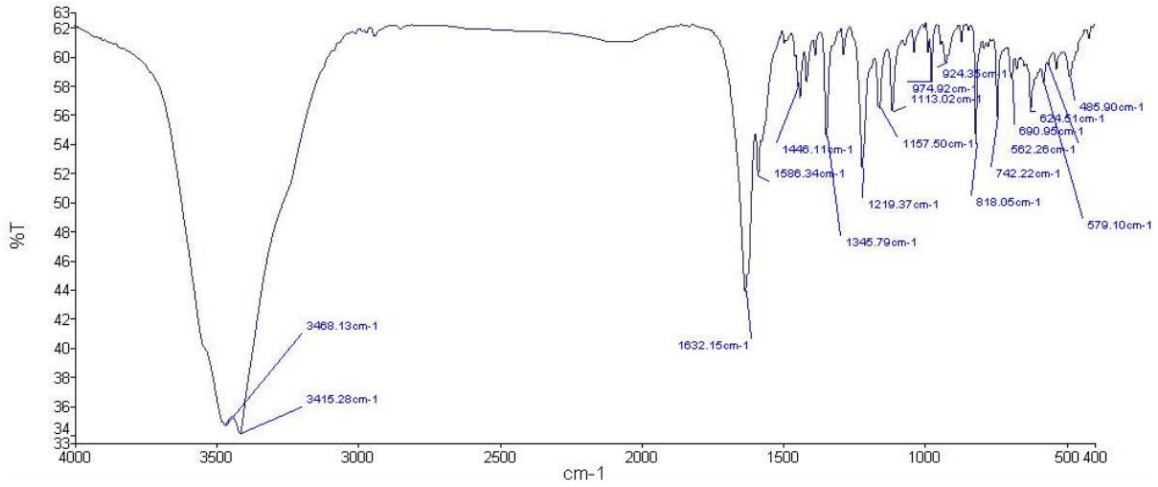

Fig. 6: FTIR spectrum of FKB loaded Ag NPs.

Conclusion

Ag NPs were successfully synthesized as indicated by the transformation of the colourless mixture to a pale-yellow colloidal solution in the chemical method. In the UV-visible spectrum, FKB showed two characteristic absorption bands centered at 300 nm and 393 nm while AgFKB NPs showed peaks at 300 nm and 421 nm. FTIR showed absorption bands at 3415.28 cm^{-1} and 3468.13 cm^{-1} (O-H stretch), 1632.15 cm^{-1} (α, β-unsaturated carbonyl group), 1586.34 cm^{-1} (aromatic C=C stretch), and 1219.37 cm^{-1} (C-O-C ether linkage). The C-H stretching that occurs above 3000 cm^{-1} also confirmed the presence of the aromatic compound. XRD exhibited a crystalline nature with reflected peaks at 2θ=38.12 and 44.31, which correspond to the (111) and (200) crystallographic planes of face-centered cubic (fcc) Ag crystals. FESEM described the crystalline nature of pure FKB with a clear and flat surface; loaded Ag NPs on the surface of FKB. The minimum inhibitory concentration of AgFKB against gram-negative bacteria, *E. coli* and *P. aeruginosa* was found to be 100 µg/mL as all the 100 µg/mL AgFKB discs showed an inhibition zone of 6 mm in diameter in the activity against *E. coli* and *P. aeruginosa*. However, 100 µg/mL FKB discs did not show any inhibition zone in the activity.

Acknowledgment

One of us (Muhammad Nadeem Akhtar) would like to acknowledge the Higher Education Commission (HEC) for the award of NRPU grant NO. 15788. We are also thankful to the Ministry of Education of Malaysia for the award of FRGS RDU 150109.

References

1. S. Srivastava and A. Bhargava, "*Green Nanotechnology: An Overview*". Green Nanoparticles: The Future of Nanobiotechnology: 1 (2022).
2. S. Ahmed, M. Ahmad, B. L. Swami, and S. Ikram, "*A review on plant extract mediated synthesis of silver nanoparticles for antimicrobial applications: a green expertise". J. Adv. Res.*, **7,** 17 (2016).
3. M. Mohsin, I. A. Bhatti, A. Ashar, M. W. Khan, M. U. Farooq, H. Khan, Mx. T. Hussain, S. Loomba, M. Mohiuddin, and A. Zavabeti, "*Iron-doped zinc oxide for photocatalyzed degradation of humic acid from municipal wastewater". Appl. Mater. Today.*, **23**, 101047 (2021).
4. L. Xing, Y. Xiahou, P. Zhang, W. Du, and H. Xia, "*Size control synthesis of monodisperse, quasi-spherical silver nanoparticles to realize surface-enhanced Raman scattering uniformity and reproducibility". ACS Appl. Mater. Interfaces.*, **11,** 17637 (2019).
5. I. Hussain, N. B. Singh, A. Singh, H. Singh, and S. C. Singh, "*Green synthesis of nanoparticles and its potential application". Biotechnol. Lett.*, **38,** 545 (2016).

6. D. Bhattacharya, B. Ghosh, and M. Mukhopadhyay, "*Development of nanotechnology for advancement and application in wound healing: a review".IET nanobiotechnol.*, **13,** 778 (2019).
7. K. A. Khalil, H. Fouad, T. Elsarnagawy, and F. N. Almajhdi, "*Preparation and Characterization of Electrospun PLGA/silver Composite Nanofibers for Biomedical Applications". Int. J. Electrochem. Sci.*, **8,** 3483 (2013).
8. S. S. Mughal and S. M. Hassan, "*Comparative Study of AgO Nanoparticles Synthesize Via Biological, Chemical and Physical Methods: A Review". Am. J. Mater. Synt. and Process.*, **7,** 15 (2022).
9. F. Afkhami, P. Forghan, J. L. Gutmann, and A. Kishen, "*Silver Nanoparticles and Their Therapeutic Applications in Endodontics: A Narrative Review". Pharm.*, **15,** 715 (2023).
10. M. R. Kalbassi, J. H. Salari, and A. Johari, "*Toxicity of silver nanoparticles in aquatic ecosystems: salinity as the main cause in reducing toxicity".* (2011).
11. M. Saravanan, S. K. Barik, D. Mubarakali, P. Prakash, and A. Pugazhendhi, "*Synthesis of silver nanoparticles from Bacillus brevis (NCIM 2533) and their antibacterial activity against pathogenic bacteria". Microb. Pathog.*, **116**: 221 (2018).
12. I. X. Yin, J. Zhang, I. S. Zhao, M. L. Mei, Q. Li, and C. H. Chu, "*The antibacterial mechanism of silver nanoparticles and its application in dentistry". Int. J. Nanomed.*, **15**: 2555 (2020).
13. S. Iravani, "*Green synthesis of metal nanoparticles using plants". Green Chem.*, **13,** 2638 (2011).
14. S. P. Deshmukh, S. Patil, S. Mullani, and S. Delekar, "*Silver nanoparticles as an effective disinfectant: A review". Mater. Sci. Eng. C*, **97**: 954 (2019).
15. S. L. Bee, Y. Bustami, A. Ul-Hamid, and Z. A. Hamid, "*Green biosynthesis of hydroxyapatite-silver nanoparticle nanocomposite using aqueous Indian curry leaf (Murraya koengii) extract and its biological properties". Mater. Chem. Phys.*, **277**: 125455 (2022).
16. A. M. Díez-Pascual, "*Recent progress in antimicrobial nanomaterials". Nanomater.*, **10,** 2315 (2020).
17. F. Ameen, A. A. Al-Homaidan, A. Al-Sabri, A. Almansob, and S. Alnadhari, "*Anti-oxidant, anti-fungal and cytotoxic effects of silver nanoparticles synthesized using marine fungus Cladosporium halotolerans". Appl. Nanosci.*, **13,** 623 (2023).
18. S. Chanda, "*Silver nanoparticles (medicinal plants mediated): A new generation of antimicrobials to combat microbial pathogens-a review".* Microbial pathogens and strategies for combating them: science, technology and education: 1314 (2013).
19. S. Gankhuyag, D. S. Bae, K. Lee, and S. Lee, "*One-pot synthesis of SiO_2@ Ag mesoporous nanoparticle coating for inhibition of Escherichia coli bacteria on various surfaces". Nanomater.*, **11**(2): 549 (2021).
20. W. Luo, L.-B. Yang, C.-C. Qian, B. Ma, G. M. Manjengwa, X.-M. Miao, J. Wang, C.-H. Hu, B. Jin, and L.-X. Zhang, "*Flavokawain B alleviates LPS-induced acute lung injury via targeting myeloid differentiation factor 2". Acta Pharmacol. Sin.*, **43**, 1758, (2022).
21. N. Abu, M. N. Akhtar, S. K. Yeap, K. L. Lim, W. Y. Ho, M. P. Abdullah, C. L. Ho, A. R. Omar, J. Ismail, and N. B. Alitheen, "*Flavokawain B induced cytotoxicity in two breast cancer cell lines, MCF-7 and MDA-MB231 and inhibited the metastatic potential of MDA-MB231 via the regulation of several tyrosine kinases In vitro". BMC Complement. Altern. Med.*, **16**, 1 (2016).
22. M. C. Rossette, D. C. Moraes, E. K. Sacramento, M. A. Romano-Silva, J. L. Carvalho, D. A. Gomes, H. Caldas, E. Friedman, L. Bastos-Rodrigues, and L. De Marco, "*The in vitro and in vivo antiangiogenic effects of flavokawain B". Phytother. Res.*, **31,** 1607 (2017).
23. N. Abu, N. E. Mohamed, S. K. Yeap, K. L. Lim, M. N. Akhtar, A. J. Zulfadli, B. B. Kee, M. P. Abdullah, A. R. Omar, and N. B. Alitheen, "*In vivo antitumor and antimetastatic effects of flavokawain B in 4T1 breast cancer cell-challenged mice". Drug Des. Dev. ther.*, **9**: 1401 (2015).
24. Y. C. Hseu, Y. C. Huang, V. Thiyagarajan, D. C. Mathew, K. Y. Lin, S. C. Chen, J. Y. Liu, L. S. Hsu, M. L. Li, and H. L. Yang, "*Anticancer activities of chalcone flavokawain B from Alpinia pricei Hayata in human lung adenocarcinoma (A549) cells via induction of reactive oxygen species-mediated apoptotic and autophagic cell death". J. Cell. Physiol.*, **234,** 17514 (2019).
25. N. Abu, M. N. Akhtar, S. K. Yeap, K. L. Lim, W. Y. Ho, A. J. Zulfadli, A. R. Omar, M. R. Sulaiman, M. P. Abdullah, and N. B. Alitheen, "*Flavokawain A induces apoptosis in MCF-7 and MDA-MB231 and inhibits the metastatic process in vitro". PLoS One*, **9,** e105244 (2014).
26. N. Abu, W. Y. Ho, S. K. Yeap, M. N. Akhtar, M. P. Abdullah, A. R. Omar, and N. B. Alitheen, "*The flavokawains: uprising medicinal chalcones". Cancer Cell Int.*, **13**, 1-7 (2013).
27. A. Abu Bakar, M. N. Akhtar, N. Mohd Ali, S. K. Yeap, C. K. Quah, W.-S. Loh, N. B. Alitheen, S. Zareen, Z. Ul-Haq, and S. a. A. Shah, "*Design, synthesis and docking studies of flavokawain B type chalcones and their cytotoxic effects on*

MCF-7 and MDA-MB-231 cell lines". Mol., **23,** 616 (2018).

28. N. Abu, N. E. Mohamed, N. Tangarajoo, S. K. Yeap, M. N. Akhtar, M. P. Abdullah, A. R. Omar, and N. B. Alitheen, "*In vitro toxicity and in vivo immunomodulatory effects of flavokawain A and flavokawain B in Balb/C mice". Nat. Prod. Commun.*, **10,** 1934578X1501000716 (2015).
29. A. Mohamad, M. Akhtar, Z. Zakaria, E. Perimal, S. Khalid, P. Mohd, M. Khalid, D. Israf, N. Lajis, and M. Sulaiman, "*Antinociceptive activity of a synthetic chalcone, flavokawin B on chemical and thermal models of nociception in mice". Eur. J. Pharmacol.*, **647,** 103 (2010).
30. T. Lu, X. Zhao, X. Li, G. Hansen, J. Blondeau, and K. Drlica, "*Effect of chloramphenicol, erythromycin, moxifloxacin, penicillin and tetracycline concentration on the recovery of resistant mutants of Mycobacterium smegmatis and Staphylococcus aureus". J. Antimicrob. Chemother.*, **52,** 61 (2003).
31. P. Khanna, N. Singh, S. Charan, V. Subbarao, R. Gokhale, and U. Mulik, "*Synthesis and characterization of Ag/PVA nanocomposite by chemical reduction method". Mater. Chem. Phys.*, **93,** 117, 121 (2005).
32. A. Pal, S. Shah, and S. Devi, "*Synthesis of Au, Ag and Au–Ag alloy nanoparticles in aqueous polymer solution". Colloids Surf. A: Physicochem. Eng. Asp.*, **302,** 51 (2007).
33. S. S. Patil, R. S. Dhumal, M. V. Varghese, A. Paradkar, and P. Khanna, "*Synthesis and antibacterial studies of chloramphenicol loaded nano-silver against Salmonella typhi". Synth. React. Inorg. Met. Org. Nano Met. Chem.*, **39,** 65 (2009).
34. D. Manisha, J. Alwala, K. R. Kudle, and M. P. Rudra, "*Biosynthesis of silver nanoparticles using flower extracts of Catharanthus roseus and evaluation of its antibacterial efficacy". World J. Pharm. Pharm. Sci.*, **3**: 877 (2014).
35. S. Mourdikoudis, R. M. Pallares, and N. T. Thanh, "*Characterization techniques for nanoparticles: comparison and complementarity upon studying nanoparticle properties". Nanoscale*, **10**(27): 12871-12934 (2018).
36. Y. Y. Loo, B. W. Chieng, M. Nishibuchi, and S. Radu, "*Synthesis of silver nanoparticles by using tea leaf extract from Camellia sinensis". Int. J. Nanomed.*, **7**, 4263 (2012).
37. X. Hu, Q. Zhu, X. Wang, N. Kawazoe, and Y. Yang, "*Nonmetal–metal–semiconductor-promoted P/Ag/Ag 2 O/Ag 3 PO 4/TiO 2 photocatalyst with superior photocatalytic activity and stability". J. Mater. Chem. A*, **3,** 17858 (2015).
38. S. Ponarulselvam, C. Panneerselvam, K. Murugan, N. Aarthi, K. Kalimuthu, and S. Thangamani, "*Synthesis of silver nanoparticles using leaves of Catharanthus roseus Linn. G. Don and their antiplasmodial activities". Asian Pac. J. Trop. Biomed.*, **2,** 574 (2012).
39. J. Zhang, Y. Li, L. Zhu, X. Wang, and J. Tu, "*Potassiophilic skeleton achieving highly stable potassium metal anode". Chem. Eng. J.*, **449**, 137659 (2022).
40. M. Mohsin, I. A. Bhatti, A. Ashar, A. Mahmood, Q. Ul Hassan, and M. Iqbal, "*Fe/ZnO@ ceramic fabrication for the enhanced photocatalytic performance under solar light irradiation for dye degradation". J. Mater. Res. Technol.*, **9,** 4218 (2020).
41. K. Shrivas, B. Sahu, M. K. Deb, S. S. Thakur, S. Sahu, R. Kurrey, T. Kant, T. K. Patle, and R. Jangde, "*Colorimetric and paper-based detection of lead using PVA capped silver nanoparticles: Experimental and theoretical approach". Microchem. J.*, **150**, 104156 (2019).
42. M. Naveed, H. Batool, S. U. Rehman, A. Javed, S. I. Makhdoom, T. Aziz, A. A. Mohamed, M. Y. Sameeh, M. W. Alruways, and A. S. Dablool, "*Characterization and evaluation of the antioxidant, antidiabetic, anti-inflammatory, and cytotoxic activities of silver nanoparticles synthesized using Brachychiton populneus leaf extract". Process.*, **10,** 1521 (2022).
43. P. Van Dong, C. H. Ha, L. T. Binh, and J. Kasbohm, "*Chemical synthesis and antibacterial activity of novel-shaped silver nanoparticles". Int. Nano Lett.*, **2,** 1 (2012).
44. H. H Rashed, "*Silver nanoparticles prepared by electrical arc discharge method in DIW". Eng. Technol. J.*, **34,** 295 (2016).
45. C. Khurana, A. K. Vala, N. Andhariya, O. Pandey, and B. Chudasama, "*Antibacterial activities of silver nanoparticles and antibiotic-adsorbed silver nanoparticles against biorecycling microbes". Environ. Sci.: Process. Impacts*, **16,** 2191 (2014).
46. M. A. Aguilar-Méndez, S. Martín-Martínez, L. Ortega-Arroyo, G. Cobián-Portillo, and E. Sánchez-Espíndola, "*Synthesis and characterization of silver nanoparticles: effect on phytopathogen Colletotrichum gloesporioides". J. Nanoparticle Res.*, **13,** 2525 (2011).
47. J. Coates, "*Interpretation of infrared spectra, a practical approach"*. 2000, Citeseer.